



Dalton
Transactions

**Facile mechanochemical synthesis of MIL-53 and its
isorecticular analogues with a glance at reaction reversibility**

Journal:	<i>Dalton Transactions</i>
Manuscript ID	DT-COM-02-2024-000372
Article Type:	Communication
Date Submitted by the Author:	06-Feb-2024
Complete List of Authors:	Salvador, Fillipp; New Mexico Institute of Mining and Technology, Chemistry Tegudeer, Zhuorigebatu; Ohio University, Chemistry and Biochemistry Locke, Halie; New Mexico Institute of Mining and Technology, Chemistry Gao, Wen-Yang; Ohio University, Chemistry and Biochemistry

SCHOLARONE™
Manuscripts

COMMUNICATION

Facile mechanochemical synthesis of MIL-53 and its isorecticular analogues with a glance at reaction reversibility

Fillipp Edvard Salvador,^{a,†} Tegudeer Zhuorigebatu,^{b,†} Halie Locke^a and Wen-Yang Gao^{*b}

Received 00th January 20xx,
Accepted 00th January 20xx

DOI: 10.1039/x0xx00000x

MIL-53 represents one of the most notable metal-organic frameworks given its unique structural flexibility and remarkable thermal stability. In this study, a shaker-type ball milling method has been developed into a facile and generalizable synthetic strategy to access a family of MIL-53 type materials under ambient conditions. During the explorations of $[M(OH)(\text{fumarate})]$ ($M = \text{Al}$, Ga , and In), we report a positive correlation between the metal–ligand (M–L) bond reversibility and the size of resultant crystallites under the mechanochemical process. The more kinetically labile the M–L bond is, the larger the afforded crystallite size is.

MIL-53 (MIL = Matériaux de l'Institut Lavoisier), one of the most widely explored metal-organic frameworks (MOFs) over the last two decades, has been well known for its structural flexibility, compositional modularity, and remarkable thermal stability.^{1, 2} Isostructural to Cr-MIL-53 initially reported in 2002,³ Al-MIL-53 consists of *trans* chains of corner sharing $\text{AlO}_4(\text{OH})_2$ octahedra linked together by 1,4-benzenedicarboxylate (bdc) ligands, ultimately forming a 3-dimensional network with rhombic channels and the formula of $[\text{Al}(\text{OH})(\text{bdc})]$ (Figure 1). Al-MIL-53 exhibits a unique structural flexibility – fully reversible between open and closed conformations – described as the breathing effect.^{4–7} The pore expansion/contraction process provides valuable opportunities to fundamentally understand dynamic changes in solid-state structures and tune the selectivity and/or diffusivity of guest molecules in MOFs during practical applications.^{8, 9}

The synthesis of MIL-53 type materials is typically accomplished by solvothermal (e.g., *N,N*-dimethylformamide

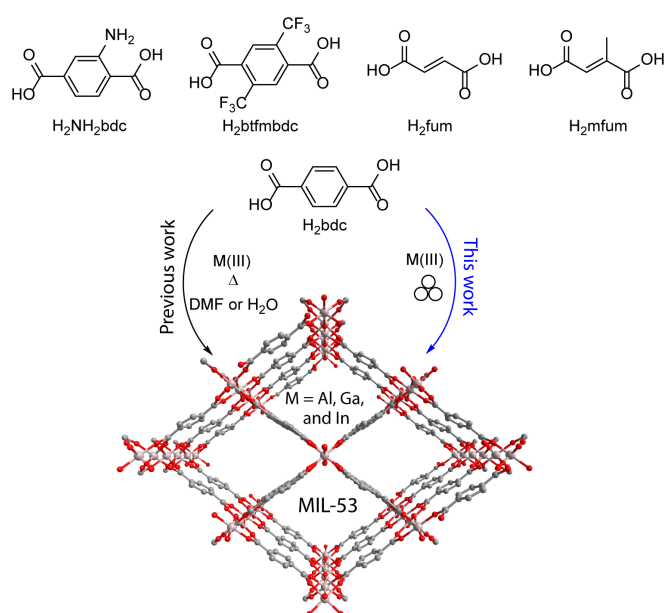


Figure 1. In contrast to the previously known solvothermal or hydrothermal reactions, this work reports a facile mechanochemical synthesis strategy to access Al-MIL-53, which is immediately generalizable to isostructures of MIL-53 based on a series of ligands, as well as other elements in group 13.

(DMF) as the solvent) or hydrothermal reactions at elevated temperature (Figure 1).^{1, 10, 11} The employment of such harsh conditions makes the reversible formation of metal–ligand (M–L) coordinate bonds possible, which thus leads to the formation of (poly)crystalline samples over periods of hours to days. Additionally, known solid-state synthesis for Cr-MIL-53 and other Al-MOFs must depend on extended thermal annealing processes ($\geq 160^\circ\text{C}$) following the initial grinding to deliver the crystallinity.^{12, 13} A direct yet facile preparation method is still highly desirable to access MIL-53 and its isorecticular analogues in a sustainable manner, given its great application potential.

Over the last decades mechanochemistry has resurged as an alternative and green synthetic strategy using commercially

^a Department of Chemistry, New Mexico Institute of Mining and Technology, Socorro, New Mexico 87801, United States.

^b Department of Chemistry and Biochemistry, Ohio University, Athens, Ohio 45701, United States. E-mail: gaow@ohio.edu

[†] These two authors contributed equally.

Electronic Supplementary Information (ESI) available: [details of mechanochemical synthesis and characterization using powder X-ray diffraction (PXRD), infrared (IR) spectroscopy, N_2 adsorption isotherms, thermogravimetric analysis (TGA), and others]. See DOI: 10.1039/x0xx00000x

available mills to build an array of MOFs with advantageous features of solvent volume reduction, high reaction yield, and easiness to scale-up.^{14, 15} Based on our long-standing interest in mechanochemistry^{16–18} and inspired by the preparation of [Al(OH)(fum)] (fum = fumarate) through a twin-screw extrusion method reported by James et al.,¹⁹ herein we report that a family of MIL-53 type materials has been successfully built by mechanochemical synthesis, more specifically a shaker-type ball milling, under ambient conditions. Not only is the developed synthetic strategy compatible with ligand variation, but it also allows us to produce gallium (Ga)- and indium (In)-based MOFs in addition to the Al congener. Moreover, a positive correlation between M–L bond reversibility kinetics and crystallite sizes has been observed for the first time and further elaborated for the solid-state mechanochemical reactions. It is worth noting that, prior to this study, there has been no known case of Al-MIL-53 or Ga-based MOFs being made through mechanochemistry.¹⁵ Previously known mechanochemistry has been primarily restrained to the (first-row) transition and rare-earth metals delivering HKUST-1,^{20, 21} MOF-5,^{22–25} ZIFs,^{26–29} MOF-74,^{30–32} pillar-layered structures,^{33, 34} UiOs,^{35–39} and others.^{40–42} However, both MIL-53 and other group 13 element-based MOFs remain rare to be accessed by direct milling.^{43, 44}

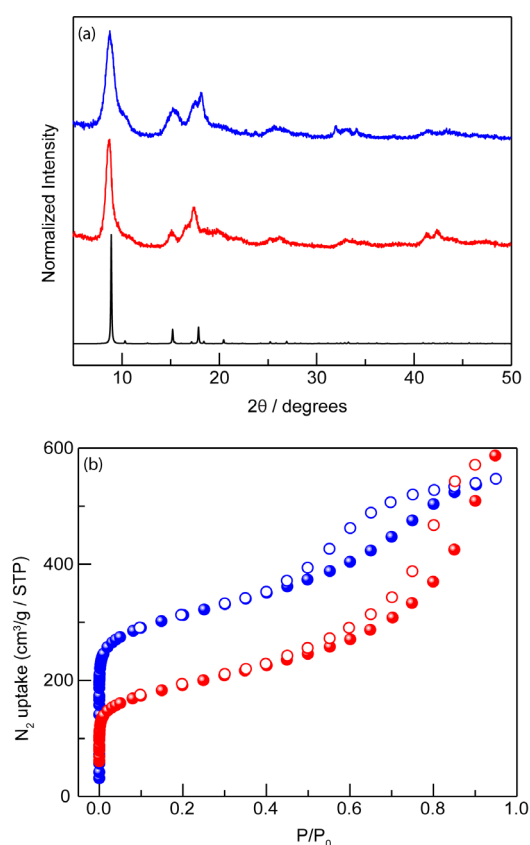


Figure 2. (a) PXRD patterns of [Al(OH)(bdc)] mechanochemically prepared by a one-pot reaction (red line) and a stepwise procedure (blue line) are compared to the calculated patterns of [Al(OH)(bdc)] (black line). (b) N_2 adsorption isotherms are collected at 77 K on the samples of [Al(OH)(bdc)] prepared by a one-pot reaction (red) and a stepwise procedure (blue).

To prepare [Al(OH)(bdc)] (Al-MIL-53) mechanochemically, we investigated a number of experimental variables systematically: 1) *aluminium(III) precursors* – milling aluminium sulfate octadecahydrate ($Al_2(SO_4)_3 \cdot 18H_2O$, 1.0 equiv), H_2bdc (2.0 equiv), and NaOH (6.0 equiv) in the presence of DMF ($\eta = 0.3 \mu L/mg$) in one pot for 1 h at a frequency of 30 Hz provides a crystalline phase, that matches the powder X-ray diffraction (PXRD) patterns from the calculated ones of MIL-53 (Figure 2a). However, the employment of $Al(OH)_3$, $Al(OH)(OAc)_2$ or $Al(NO_3)_3 \cdot 9H_2O$ instead of $Al_2(SO_4)_3 \cdot 18H_2O$, does not generate the desired phase under similar conditions (Figure S1 in Electronic Supplementary Information, ESI). We tentatively attribute this phenomenon to the release of relatively abundant water molecules from $Al_2(SO_4)_3 \cdot 18H_2O$ in the solid mixture, which facilitates the milling reaction. The dissociation of labile aqua ligands along with non-coordinating SO_4^{2-} anions⁴⁵ makes Al(III) sites readily available for carboxylate bonding compared to coordinated hydroxide or acetate. 2) *liquid additive* – the addition of DMF in an appropriate amount ($\eta = 0.30\text{--}0.45 \mu L/mg$) also matters to the formation of MIL-53 – no mechanochemical reaction proceeds under the neat condition and replacing DMF with either H_2O or MeOH generates poor crystalline phases (Figures S2 and S3). We suspect a DMF-derived microenvironment, which dissolves reagents and promotes their mobility, is necessary for the formation of Al-MIL-53. 3) *milling time* – the mechanochemical reaction is complete after milling for 1 h at 30 Hz and the extension of milling time leads to the broadening of PXRD peaks (Figure S4). 4) *one-pot vs. stepwise reaction* – a much higher surface area ($1143 \text{ m}^2/\text{g}$, $P/P_0 = 0.007\text{--}0.03$) is observed from a stepwise approach than that ($666 \text{ m}^2/\text{g}$, $P/P_0 = 0.007\text{--}0.03$) of the one-pot method based on their N_2 adsorption isotherms at 77 K (Figure 2b), though PXRD patterns collected from the two samples look comparable to each other (Figure 2a). The pre-milling of H_2bdc and NaOH before adding $Al_2(SO_4)_3 \cdot 18H_2O$ and DMF allows us to reach a surface area value comparable to the hydrothermally prepared sample.¹ The enhancement in material quality is tentatively attributed to a great degree of ligand deprotonation from the initial milling leading to the

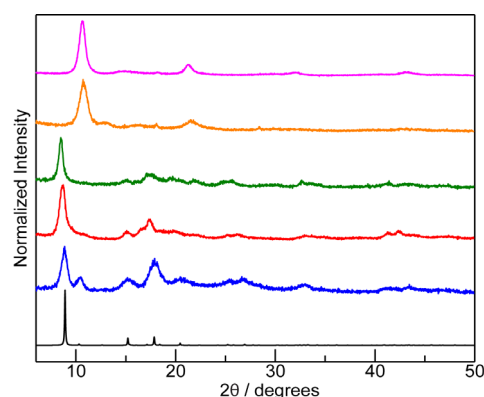


Figure 3. PXRD patterns of mechanochemically prepared [Al(OH)(fum)] (magenta), [Al(OH)(mfum)] (orange), [Al(OH)(btmbdc)] (olive), [Al(OH)(bdc)] (red), and [Al(OH)(NH₂bdc)] (blue) were collected and compared to the calculated PXRD patterns of [Al(OH)(bdc)] (black line), which indicates they are all isostructural to MIL-53.

presence of rich bdc anions, which can readily coordinate with Al(III) to form the extended lattice.

Further characterizations were also carried out on the mechanochemically obtained [Al(OH)(bdc)]. The completeness of the reaction was monitored by infrared (IR) spectroscopy (Figure S5) – the disappearance of the uncoordinated carbonyl stretch at around 1675 cm^{-1} indicates the absence of free H_2bdc , while bands around 1410 cm^{-1} and 1600 cm^{-1} , corresponding to $-\text{CO}_2$ asymmetric and symmetric stretching, are characteristic to the coordinated carboxylate group and indicate its presence in the product. The thermogravimetric analysis (TGA, Figure S6) indicates that [Al(OH)(bdc)] prepared by ball milling exhibits a continuous weight loss prior to $100\text{ }^\circ\text{C}$ corresponding to the removal of guest molecules and then keeps its stability up to $520\text{ }^\circ\text{C}$, which is consistent with the reported thermal behaviour of the solvothermally generated MIL-53.¹

We extended the above mechanochemical synthetic method to generate [Al(OH)(fum)],⁴⁶ isostructural to MIL-53. We have found that milling $\text{Al}_2(\text{SO}_4)_3 \cdot 18\text{H}_2\text{O}$ (1.0 equiv) and fumaric acid (H_2fum , 2.0 equiv) with a stoichiometric amount of sodium hydroxide (NaOH, 6.0 equiv) as well as a small amount of DMF ($\eta = 0.30\text{ }\mu\text{L/mg}$) for 90 minutes affords the desired crystalline phase of [Al(OH)(fum)] (Figure 3, experimental details in ESI). The added NaOH deprotonates fumaric acid and

provides hydroxide anions to complete $\text{AlO}_4(\text{OH})_2$ octahedra, similar to its role in the synthesis of [Al(OH)(bdc)]. No mechanochemical polymerization was observed in the absence of NaOH, evidenced by the reaction mixture being completely dissolved in water during the workup. Meanwhile, unlike the mechanochemical synthesis of [Al(OH)(bdc)] that is sensitive to the additive liquid (DMF), [Al(OH)(fum)] is readily accessible regardless of additives – the neat condition or adding DMF ($\eta = 0.30 - 1.5\text{ }\mu\text{L/mg}$), MeOH ($\eta = 0.30\text{ }\mu\text{L/mg}$), or H_2O ($\eta = 0.30\text{ }\mu\text{L/mg}$) consistently generates [Al(OH)(fum)] (Figures S7–S9). Other characterization data, e.g., IR (Figure S10), TGA (Figure S11), and N_2 adsorption isotherms (Figure S12) included in ESI, are consistent with those of the reported solvothermally prepared sample.^{19, 46, 47}

The developed mechanochemical process exhibits great tolerance towards a series of different functional groups, when preparing other Al-based MOFs, [Al(OH)L] ($\text{H}_2\text{L} = 2\text{-aminobenzene-1,4-dicarboxylic acid (H}_2\text{NH}_2\text{bdc)}$, $2,5\text{-bis(trifluoromethyl)benzene-1,4-dicarboxylic acid (H}_2\text{btfmbdc)}$, and $2\text{-methylfumaric acid (H}_2\text{mfum)}$). We have found the milling method produces crystalline materials of [Al(OH)(NH₂bdc)] (Figures S13–S18), [Al(OH)(btfmbdc)] (Figures S19–S23), and [Al(OH)(mfum)] (Figures S24–S28) (reaction and characterization details in ESI), which are isostructural to MIL-53 confirmed by PXRD (Figure 3). The completeness of the mechanochemical reactions was similarly monitored by IR (Figures S16, S22, and S26) and the obtained materials were also characterized by TGA (Figures S18, S23, and S28) and N_2 adsorption analysis (Figures S17 and S27). While all milling reactions proceeded at a stoichiometric 1:2 molar ratio of $\text{Al}_2(\text{SO}_4)_3 \cdot 18\text{H}_2\text{O}$ and the ligand, slight variations are necessary to generate the quality crystalline phases regarding reaction time, the additive liquid, and its amount.

Beyond Al(III) being employed as the metal node of MOFs, we have discovered that other group 13 elements-based MOFs, [M(OH)(fum)] ($\text{M} = \text{Ga or In}$), enable their mechanochemical access for the first time, confirmed by PXRD (Figure 4a) and other characterizations (Figures S29–S36). These two materials were previously prepared by solvothermal methods.⁴⁸ The trivalent cations Al(III), Ga(III), and In(III) featuring closed shell electron configurations follow an increasing trend in their ionic radii ($53 < 62 < 80\text{ pm}$), which leads to the expansion of MOF lattice parameter consistently reflected by the observable shifting of PXRD peaks towards low angles (Figure 4a). Moreover, dramatic differences of peak width show up in those PXRD patterns, particularly between [Al(OH)(fum)] and the other two. The crystallite sizes of [M(OH)(fum)] ($\text{M} = \text{Al, Ga, and In}$) are calculated to be $13(3)\text{ nm}$, $39(4)\text{ nm}$, and $49(2)\text{ nm}$, respectively, based on these PXRD patterns and Scherrer equation.⁴⁹ Although we recognize various factors may contribute to the observed PXRD peak width entangled by the milling process, the discrepancy of crystallite sizes among the three MOFs should still be appreciated and is worth further discussion.

Crystalline MOF formation counts on the reversibility of M–L coordinate bonds during the chemical reactions regardless of solution or solid state.^{16, 50} Thus, the M–L bond lability plays a

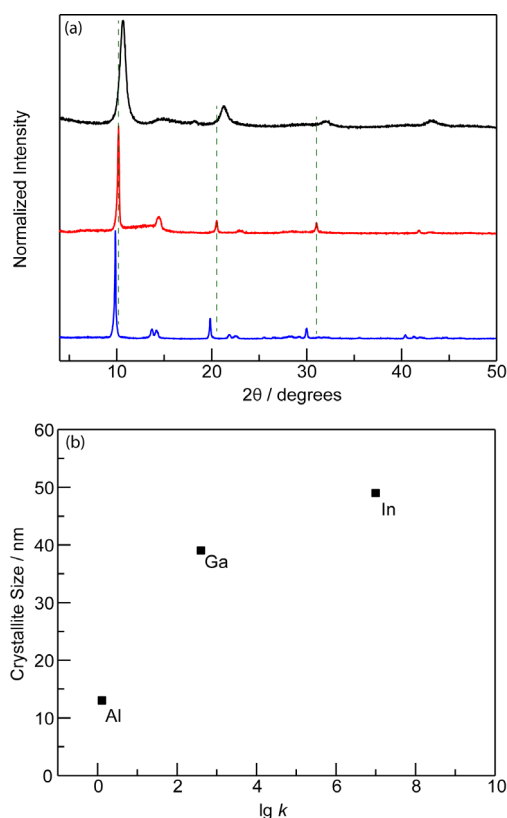


Figure 4. (a) PXRD patterns of the mechanochemically obtained [Al(OH)(fum)] (black line), [Ga(OH)(fum)] (red line), and [In(OH)(fum)] (blue line) are compared. As we move down in group 13 of the periodic table, PXRD peaks systematically shift towards low angles indicated by the dotted lines and the diffraction peak width is consistently decreasing. (b) a positive correlation is presented between the crystallite size and the metal-ligand reversibility. The metal-ligand reversibility is indicated by the water exchange rate constants (k/s^{-1}) previously reported for aquated trivalent metal cations.

critical role in mechanochemical reaction kinetics and is expected to guide the growth of lattice in its size and quality. To gauge the reversibility of metal–oxygen (M–O) dative bonds in the (near) solid-state mechanochemical reactions, we propose to employ water exchange rate constants of aquated metal ions in aqueous solutions as a conceptual model. The water exchange rate constants (k / s^{-1} at 298 K) were experimentally measured and reported as 1.29 s^{-1} for Al(III)⁵¹ and $4 \times 10^2 \text{ s}^{-1}$ for Ga(III),⁵² in addition to In(III) having a predicted value of around 10^7 s^{-1} caused by difficulties in measuring its fast exchange.⁵³ A positive correlation between the crystallite sizes and the water exchange rate constants is thus presented (Figure 4b). The more labile the M–L bond is, the bigger crystallite size the reaction affords under similarly optimized mechanochemical conditions. The borderline water exchange rate of Al(III) between kinetic inertness and lability truly challenges the access to large crystallite sizes of Al-based MOFs. This also explains suitable-size crystals of Al-MOFs are typically rare for single-crystal X-ray diffraction even in the solvothermal reaction systems.²

As we know, larger ions have faster ligand exchange rates due to decreasing electrostatic attractions. During the mechanochemical formation of extended MOF lattices, other factors that need to be considered regarding the reversibility of M–L connection include milling time duration and the number of the ligand binding sites. On one hand, the slow kinetics of Al(III) manifests in the extended 90-min milling time to access the quality [Al(OH)(fum)], while Ga and In analogues only require 45-min reaction time. However, it is obvious to envision the constant and extended milling can break down generated large-size crystallites, leading to the broadening of PXRD peak width. On the other hand, the reversibility of M–L connection can be impeded by a high number of ligand binding sites specially at ambient temperature. Mechanochemistry rarely delivers MOFs based on the ligands containing hexacarboxylic acid or more.^{16, 54, 55} This may be rationalized by rather sluggish M–L reversibility owing to the multiple binding sites, while productive M–L reversibility demands high mechanical energy input simultaneously being detrimental to anticipated quality crystallites in size.

In summary, we report the development of a mechanochemical method for the synthesis of a family of MOFs based on Al(III), Ga(III), and In(III) sharing the same topology with MIL-53. The described mechanochemical synthetic process features remarkable sustainable features, including short reaction time, ambient reaction temperature, and (near) solvent free conditions. The mechanochemical strategy is generalizable to ligands owning different functional groups and enables access to various isostructures, including [Al(OH)(NH₂bdc)], [Al(OH)(btmbdc)], [Al(OH)(fum)], and [Al(OH)(mfum)], in addition to [Al(OH)(bdc)]. Moreover, a positive correlation between the metal–ligand (M–L) reversibility (gauged by water exchange rate constants in aquated metal complexes) and the size of resultant crystallites is observed. The kinetic lability of the M–L bond leads to increasing crystallite size in the solid-state mechanochemistry. We expect this conceptual correlation can be applied to other

types of crystal growth process, where the formation of extended lattices is ruled by the evolution of M–L bonds.

Acknowledgements

This material is based upon work supported by the National Science Foundation under Grant No. [2345469]. Exploratory studies of the mechanochemistry were supported by the start-up funds of New Mexico Tech and Ohio University.

There are no conflicts to declare.

References

- 1 T. Loiseau, C. Serre, C. Huguenard, G. Fink, F. Taulelle, M. Henry, T. Bataille and G. Férey, A Rationale for the Large Breathing of the Porous Aluminum Terephthalate (MIL-53) Upon Hydration. *Chem. Eu. J.*, 2004, **10**, 1373.
- 2 F. Millange and R. I. Walton, MIL-53 and its Isorecticular Analogues: a Review of the Chemistry and Structure of a Prototypical Flexible Metal–Organic Framework. *Isr. J. Chem.*, 2018, **58**, 1019.
- 3 K. Barthelet, J. Marrot, D. Riou and G. Férey, A Breathing Hybrid Organic–Inorganic Solid with Very Large Pores and High Magnetic Characteristics. *Angew. Chem. Int. Ed.*, 2002, **41**, 281.
- 4 T. Kundu, M. Wahiduzzaman, B. B. Shah, G. Maurin and D. Zhao, Solvent-Induced Control over Breathing Behavior in Flexible Metal–Organic Frameworks for Natural-Gas Delivery. *Angew. Chem. Int. Ed.*, 2019, **58**, 8073.
- 5 A. S. Munn, R. S. Pillai, S. Biswas, N. Stock, G. Maurin and R. I. Walton, The flexibility of modified-linker MIL-53 materials. *Dalton Trans.*, 2016, **45**, 4162.
- 6 S. Biswas, T. Ahnfeldt and N. Stock, New Functionalized Flexible Al-MIL-53-X (X = -Cl, -Br, -CH₃, -NO₂, -(OH)₂) Solids: Syntheses, Characterization, Sorption, and Breathing Behavior. *Inorg. Chem.*, 2011, **50**, 9518.
- 7 G. Férey and C. Serre, Large breathing effects in three-dimensional porous hybrid matter: facts, analyses, rules and consequences. *Chem. Soc. Rev.*, 2009, **38**, 1380.
- 8 J. Y. Kim, L. Zhang, R. Balderas-Xicohtencatl, J. Park, M. Hirscher, H. R. Moon and H. Oh, Selective Hydrogen Isotope Separation via Breathing Transition in MIL-53(Al). *J. Am. Chem. Soc.*, 2017, **139**, 17743.
- 9 A. Lopez-Olvera, J. A. Zarate, E. Martinez-Ahumada, D. Fan, M. L. Diaz-Ramirez, P. A. Saenz-Cavazos, V. Martis, D. R. Williams, E. Sanchez-Gonzalez, G. Maurin and I. A. Ibarra, SO₂ Capture by Two Aluminum-Based MOFs: Rigid-like MIL-53(Al)-TDC versus Breathing MIL-53(Al)-BDC. *ACS Appl. Mater. Interfaces*, 2021, **13**, 39363.
- 10 M. Gaab, N. Trukhan, S. Maurer, R. Gummaraju and U. Muller, The progression of Al-based metal-organic frameworks – From academic research to industrial production and applications. *Microporous Mesoporous Mater.*, 2012, **157**, 131.
- 11 J. Li, V. G. Goncharov, A. C. Strzelecki, H. Xu, X. Guo and Q. Zhang, Energetic Systematics of Metal–Organic Frameworks: A Case Study of Al(III)-Trimesate MOF Isomers. *Inorg. Chem.*, 2022, **61**, 15152.
- 12 L. Han, J. Zhang, Y. Mao, W. Zhou, W. Xu and Y. Sun, Facile and Green Synthesis of MIL-53(Cr) and Its Excellent Adsorptive Desulfurization Performance. *Ind. Eng. Chem. Res.*, 2019, **58**, 15489.

- 13 J. Li, M. J. Hurlock, V. G. Goncharov, X. Li, X. Guo and Q. Zhang, Solvent-Free and Phase-Selective Synthesis of Aluminum Trimesate Metal–Organic Frameworks. *Inorg. Chem.*, 2021, **60**, 4623.
- 14 A. V. Desai, E. Lizundia, A. Laybourn, D. N. Rainer, A. R. Armstrong, R. E. Morris, S. Wuttke and R. Ettlinger, Green Synthesis of Reticular Materials. *Adv. Funct. Mater.*, 2023, 2304660.
- 15 S. Główniak, B. Szcześniak, J. Choma and M. Jaroniec, Mechanochemistry: Toward green synthesis of metal–organic frameworks. *Mater. Today*, 2021, **46**, 109.
- 16 W.-Y. Gao, A. Sur, C.-H. Wang, G. R. Lorz, A. M. Antonio, G. A. Taggart, A. A. Ezazi, N. Bhuvanesh, E. D. Bloch and D. C. Powers, Atomically Precise Crystalline Materials Based on Kinetically Inert Metal Ions via Reticular Mechanopolymerization. *Angew. Chem. Int. Ed.*, 2020, **59**, 10878.
- 17 F. E. Salvador, J. O. Barajas and W.-Y. Gao, Mechanochemical Access to Catechol-Derived Metal–Organic Frameworks. *Inorg. Chem.*, 2023, **62**, 3333.
- 18 F. E. Salvador, V. Miller, K. Shimada, C.-H. Wang, J. Wright, M. Das, Y.-P. Chen, Y.-S. Chen, C. Sheehan, W. Xu, G. Rubasinghege and W.-Y. Gao, Mechanochemistry of Group 4 Element-Based Metal–Organic Frameworks. *Inorg. Chem.*, 2021, **60**, 16079.
- 19 D. Crawford, J. Casaban, R. Haydon, N. Giri, T. McNally and S. L. James, Synthesis by extrusion: continuous, large-scale preparation of MOFs using little or no solvent. *Chem. Sci.*, 2015, **6**, 1645.
- 20 M. Klimakow, P. Klobes, A. F. Thünemann, K. Rademann and F. Emmerling, Mechanochemical Synthesis of Metal–Organic Frameworks: A Fast and Facile Approach toward Quantitative Yields and High Specific Surface Areas. *Chem. Mater.*, 2010, **22**, 5216.
- 21 X. Sun, H. Li, Y. Li, F. Xu, J. Xiao, Q. Xia, Y. Li and Z. Li, A novel mechanochemical method for reconstructing the moisture-degraded HKUST-1. *Chem. Commun.*, 2015, **51**, 10835.
- 22 D. Prochowicz, K. Sokółowski, I. Justyniak, A. Kornowicz, D. Fairen-Jimenez, T. Friščić and J. Lewiński, A mechanochemical strategy for IRMOF assembly based on pre-designed oxo-zinc precursors. *Chem. Commun.*, 2015, **51**, 4032.
- 23 D. Prochowicz, J. Nawrocki, M. Terlecki, W. Marynowski and J. Lewiński, Facile Mechanochemical Synthesis of the Archetypal Zn-Based Metal–Organic Frameworks. *Inorg. Chem.*, 2018, **57**, 13437.
- 24 S. Abedi, A. A. Tehrani and A. Morsali, Mechanochemical synthesis of isorecticular metal–organic frameworks and comparative study of their potential for nitrobenzene sensing. *New J. Chem.*, 2015, **39**, 5108.
- 25 D. Lv, Y. Chen, Y. Li, R. Shi, H. Wu, X. Sun, J. Xiao, H. Xi, Q. Xia and Z. Li, Efficient Mechanochemical Synthesis of MOF-5 for Linear Alkanes Adsorption. *J. Chem. Eng. Data*, 2017, **62**, 2030.
- 26 K. Imawaka, M. Sugita, T. Takewaki and S. Tanaka, Mechanochemical synthesis of bimetallic CoZn-ZIFs with sodalite structure. *Polyhedron*, 2019, **158**, 290.
- 27 P. J. Beldon, L. Fábán, R. S. Stein, A. Thirumurugan, A. K. Cheetham and T. Friščić, Rapid Room-Temperature Synthesis of Zeolitic Imidazolate Frameworks by Using Mechanochemistry. *Angew. Chem. Int. Ed.*, 2010, **49**, 9640.
- 28 I. Brekalo, W. Yuan, C. Mottillo, Y. Lu, Y. Zhang, J. Casaban, K. T. Holman, S. L. James, F. Duarte, P. A. Williams, K. D. M. Harris and T. Friščić, Manometric real-time studies of the mechanochemical synthesis of zeolitic imidazolate frameworks. *Chem. Sci.*, 2020, **11**, 2141.
- 29 S. Tanaka, K. Kida, T. Nagaoka, T. Ota and Y. Miyake, Mechanochemical dry conversion of zinc oxide to zeolitic imidazolate framework. *Chem. Commun.*, 2013, **49**, 7884.
- 30 J. Beamish-Cook, K. Shankland, C. A. Murray and P. Vaqueiro, Insights into the Mechanochemical Synthesis of MOF-74. *Cryst. Growth Des.*, 2021, **21**, 3047.
- 31 Z. Wang, Z. Li, M. Ng and P. J. Milner, Rapid mechanochemical synthesis of metal–organic frameworks using exogenous organic base. *Dalton Trans.*, 2020, **49**, 16238.
- 32 P. A. Julien, K. Užarević, A. D. Katsenis, S. A. Kimber, T. Wang, O. K. Farha, Y. Zhang, J. Casaban, L. S. Germann, M. Etter, R. E. Dinnebier, S. L. James, I. Halasz and T. Friščić, In Situ Monitoring and Mechanism of the Mechanochemical Formation of a Microporous MOF-74 Framework. *J. Am. Chem. Soc.*, 2016, **138**, 2929.
- 33 Y. Chen, H. Wu, Y. Yuan, D. Lv, Z. Qiao, D. An, X. Wu, H. Liang, Z. Li and Q. Xia, Highly rapid mechanochemical synthesis of a pillar-layer metal-organic framework for efficient CH₄/N₂ separation. *Chem. Eng. J.*, 2020, **385**, 123836.
- 34 T. Friščić, D. G. Reid, I. Halasz, R. S. Stein, R. E. Dinnebier and M. J. Duer, Ion- and Liquid-Assisted Grinding: Improved Mechanochemical Synthesis of Metal–Organic Frameworks Reveals Salt Inclusion and Anion Templating. *Angew. Chem. Int. Ed.*, 2010, **49**, 712.
- 35 K. Užarević, T. C. Wang, S.-Y. Moon, A. M. Fidelli, J. T. Hupp, O. K. Farha and T. Friščić, Mechanochemical and solvent-free assembly of zirconium-based metal-organic frameworks. *Chem. Commun.*, 2016, **52**, 2133.
- 36 H. Ali-Moussa, R. N. Amador, J. Martinez, F. Lamaty, M. Carboni and X. Bantreil, Synthesis and post-synthetic modification of UiO-67 type metal-organic frameworks by mechanochemistry. *Mater. Lett.*, 2017, **197**, 171.
- 37 Y.-H. Huang, W.-S. Lo, Y.-W. Kuo, W.-J. Chen, C.-H. Lin and F.-K. Shieh, Green and rapid synthesis of zirconium metal-organic frameworks via mechanochemistry: UiO-66 analog nanocrystals obtained in one hundred seconds. *Chem. Commun.*, 2017, **53**, 5818.
- 38 B. Karadeniz, A. J. Howarth, T. Stolar, T. Islamoglu, I. Dejanović, M. Tireli, M. C. Wasson, S.-Y. Moon, O. K. Farha, T. Friščić and K. Užarević, Benign by Design: Green and Scalable Synthesis of Zirconium UiO-Metal–Organic Frameworks by Water-Assisted Mechanochemistry. *ACS Sustainable Chem. Eng.*, 2018, **6**, 15841.
- 39 B. Karadeniz, D. Žilić, I. Huskić, L. S. Germann, A. M. Fidelli, S. Muratović, I. Lončarić, M. Etter, R. E. Dinnebier, D. Barišić, N. Cindro, T. Islamoglu, O. K. Farha, T. Friščić and K. Užarević, Controlling the Polymorphism and Topology Transformation in Porphyrinic Zirconium Metal–Organic Frameworks via Mechanochemistry. *J. Am. Chem. Soc.*, 2019, **141**, 19214.
- 40 N. K. Singh, M. Hardi and V. P. Balema, Mechanochemical synthesis of an yttrium based metal–organic framework. *Chem. Commun.*, 2013, **49**, 972.
- 41 A. Pichon, A. Lazuen-Garay and S. L. James, Solvent-free synthesis of a microporous metal-organic framework. *CrystEngComm*, 2006, **8**, 211.
- 42 W. Yuan, J. O'Connor and S. L. James, Mechanochemical synthesis of homo- and hetero-rare-earth(III) metal–organic frameworks by ball milling. *CrystEngComm*, 2010, **12**, 3515.
- 43 S. Tomar and V. K. Singh, Review on synthesis and application of MIL-53. *Mater. Today Proc.*, 2021, **43**, 3291.
- 44 Y. Chen, J. Xiao, D. Lv, T. Huang, F. Xu, X. Sun, H. Xi, Q. Xia and Z. Li, Highly efficient mechanochemical synthesis of an indium based metal-organic framework with excellent water stability. *Chem. Eng. Sci.*, 2017, **158**, 539.
- 45 I. A. Kirilenko, Water–Electrolyte Glass-Forming Systems: A Review. *Russ. J. Inorg. Chem.*, 2018, **63**, 1731.
- 46 E. Alvarez, N. Guillou, C. Martineau, B. Bueken, B. Van de Voorde, C. Le Guillouzer, P. Fabry, F. Nouar, F. Taulelle, D. de Vos, J. S. Chang, K. H. Cho, N. Ramsahye, T. Devic, M. Daturi, G. Maurin and C. Serre, The Structure of the Aluminum

- Fumarate Metal–Organic Framework A520. *Angew. Chem. Int. Ed.*, 2015, **54**, 3664.
- 47 J. A. Coelho, A. M. Ribeiro, A. F. P. Ferreira, S. M. P. Lucena, A. E. Rodrigues and D. C. S. de Azevedo, Stability of an Al-Fumarate MOF and Its Potential for CO₂ Capture from Wet Stream. *Ind. Eng. Chem. Res.*, 2016, **55**, 2134.
 - 48 Y. Zhang, B. E. G. Lucier, S. M. McKenzie, M. Arhangelskis, A. J. Morris, T. Friscic, J. W. Reid, V. V. Tersikh, M. Chen and Y. Huang, Welcoming Gallium- and Indium-Fumarate MOFs to the Family: Synthesis, Comprehensive Characterization, Observation of Porous Hydrophobicity, and CO₂ Dynamics. *ACS Appl. Mater. Interfaces*, 2018, **10**, 28582.
 - 49 J. I. Langford and A. J. C. Wilson, Scherrer after sixty years: A survey and some new results in the determination of crystallite size. *J. Appl. Crystallogr.*, 1978, **11**, 102.
 - 50 J. Han, X. He, J. Liu, R. Ming, M. Lin, H. Li, X. Zhou and H. Deng, Determining factors in the growth of MOF single crystals unveiled by *in situ* interface imaging. *Chem*, 2022, **8**, 1637.
 - 51 D. Hugi-Cleary, L. Helm and A. E. Merbach, Variable-Temperature and Variable-Pressure ¹⁷O-NMR Study of Water Exchange of Hexaaquaaluminium(III). *Helv. Chim. Acta*, 1985, **68**, 545.
 - 52 D. Hugi-Cleary, L. Helm and A. E. Merbach, Water Exchange on Hexaaquagallium(III): High-Pressure Evidence for a Dissociative Interchange Exchange Mechanism. *J. Am. Chem. Soc.*, 1987, **109**, 4444.
 - 53 L. Helm and A. E. Merbach, Water exchange on metal ions: experiments and simulations. *Coord. Chem. Rev.*, 1999, **187**, 151.
 - 54 F. Afshariazar and A. Morsali, The unique opportunities of mechanosynthesis in green and scalable fabrication of metal–organic frameworks. *J. Mater. Chem. A*, 2022, **10**, 15332.
 - 55 C.-A. Tao and J.-F. Wang, Synthesis of Metal Organic Frameworks by Ball-Milling. *Crystals*, 2020, **11**, 15.